

# The Role of Dislocations for the Plastic Deformation of Semicrystalline Polymers as Investigated by Multireflection X-Ray Line Profile Analysis

Florian Spieckermann, Gerald Polt, Harald Wilhelm, Michael Kerber, Erhard Schafner, Michael J. Zehetbauer

Research Group Physics of Nanostructured Materials, Faculty of Physics, University of Vienna, Boltzmannngasse 5, A-1090 Vienna, Austria

Received 30 November 2011; accepted 30 November 2011  
DOI 10.1002/app.36570  
Published online in Wiley Online Library (wileyonlinelibrary.com).

**ABSTRACT:** Wide angle X-ray experiments evaluated by recent developments of X-ray line profile analysis allow for the detection of the presence of dislocations as well as to determine their density in crystalline materials. The application to semicrystalline polymers not only provides information on the crystal size and the dislocations but—in combination with *in situ* deformation—also information on the evolution of these microstructural parameters. Investigations on cold rolled and on uniaxially compressed samples of  $\alpha$ -phase isotactic polypropylene ( $\alpha$ -iPP) as

well as poly(3-hydroxybutyrate) (P3HB) are presented. The synchrotron experiments reveal a dislocation governed deformation process in  $\alpha$ -iPP. P3HB, however, deforms by a process not including dislocation generation. Here, microcracking and strain localization in the amorphous phase seem to be the predominant deformation mechanisms. © 2012 Wiley Periodicals, Inc. *J Appl Polym Sci* 000: 000–000, 2012

**Key words:** polypropylene; polyhydroxybutyrate; plasticity; dislocations

## INTRODUCTION

The plastic deformation of semicrystalline polymers as polyethylene (PE), polypropylene (PP), polyamide (PA), and others has been thoroughly investigated in the last 50 years. The complex morphology of the material on the one hand, and the lack of appropriate experimental tools on the other hand are the main reasons why the underlying processes are not fully identified yet.

A long-lasting scientific discussion is related to the deformation mechanisms of the crystalline phase. The controversial points of view suggested crystallographic slip carried by thermally generated dislocations<sup>1,2</sup> on one side, opposed by a mechanism of adiabatic melting and recrystallization on the other.<sup>3</sup> In a critical review, Séguéla<sup>4</sup> discusses the experimental evidence leading to both concepts. On the basis of a considerable number of direct experimental evidence in the literature, this review<sup>4</sup> concludes that the governing process is indeed crystallographic slip by dislocation motion. Adiabatic melting is not fully excluded

but rather a side effect of the plastic drawing while the main carriers of plasticity are crystal slip and lamellar fragmentation. In recent scanning electron microscopy (SEM) investigations of thick PE lamellae, Galeski et al.<sup>5</sup> not only found direct evidence of grown-in screw dislocations, but also slip traces of deformation-induced dislocations were identified in the SEM by a careful optimization of the etching procedure.

Another example of direct experimental evidence for the presence and dynamic formation of dislocations during plastic deformation came from the evaluation of the whole shapes of multiple orders of X-ray line profiles.<sup>6–8</sup> The availability of high flux synchrotron radiation and progress in resolution of X-ray detection together with improvements in the available computing power allowed for reliable evaluation of the physical causes of X-ray line profile broadening.<sup>9</sup> In the present article, the theoretical background of this method is sketched and examples for the detection and evolution of the dislocation density in the melt crystallized polymers polypropylene and poly(3-hydroxybutyrate) are given and supplied with new experimental results.

Correspondence to: F. Spieckermann (florian.spieckermann@univie.ac.at).

Contract grant sponsor: University of Vienna; Austrian Science Fund FWF; contract grant number: P22913.

## FUNDAMENTALS OF MULTIPLE X-RAY LINE PROFILE ANALYSIS

The broadening of an intensity profile of a Bragg reflection in general can be described by the

convolution of the intensity profile related to the limited size of the diffracting crystal and the profile related to lattice distortions. The Fourier transform of this convolution can be written as the Warren and Averbach equation<sup>10,11</sup>

$$A(L) = A^S(L)A^D(L), \quad (1)$$

where  $L$  is the variable of the Fourier transform, and  $A^S(L)$  and  $A^D(L)$  are the size and distortion coefficients, respectively. The size distribution can be modeled with an assumed log-normal distribution included in the mathematical formulation of  $A^S(L)$ . The anisotropy of the crystal shape can be approximated by the assumption of elliptically shaped crystallites. The size broadening for the anisotropic case differs from isotropic spherical crystals in so far that the median  $m$  of the size distribution depends on the diffraction order, i.e., the Miller indices ( $hkl$ ). The strain broadening coefficient  $A^D(L)$  as calculated by Warren and Averbach depends on the length of the diffraction vector  $g$  and on the mean square strain  $\langle \varepsilon_L^2 \rangle$ . Based on experimental investigations,<sup>12-14</sup> the major part of the peak broadening caused by the mean square strain could be attributed to dislocations. This relation reads as

$$\langle \varepsilon_L^2 \rangle = \left( \frac{b}{2\pi} \right)^2 \pi \rho C_f \left( \frac{l}{R_e} \right), \quad (2)$$

where  $C$  represents the dislocation contrast factor, which determines the influence of dislocations to the diffraction profile. The values of  $C$  depend on the relative orientation between the Burgers vector  $b$ , the line vector  $l$ , and the diffraction vector  $g$ , similar to the contrast of dislocations in electron microscopy. Other parameters in eq. (2) are the average dislocation density  $\rho$  and the Wilkens function  $f$ . In single crystals,  $C$  can be determined by the knowledge of the elastic constants of the material. In polycrystals, however, only a mean contrast factor  $\bar{C}$  is obtained by averaging all possible slip systems. The most advanced versions of X-ray line profile analysis describe the characteristic broadening of several reflection orders and their upper harmonics, and are thus called MXPA (multireflection X-ray line profile analysis).<sup>9,15</sup> Different lattice defects with individual microstrain distributions cause a typical diffraction order-dependent broadening which allows to identify the nature of these defects.

The introduction of MXPA enabled a careful separation of the size broadening from that of the strain (dislocation) broadening, thus for a more reliable determination of the crystal size.<sup>16</sup> Since then MXPA has been used for the determination of crystallite sizes and inherent defects and the respective distributions/arrangements in a huge number of materi-

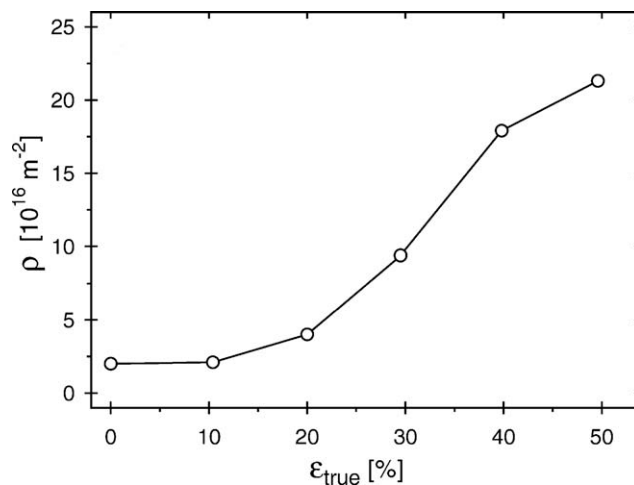


**Figure 1** Evolution of the dislocation density in  $\alpha$ -iPP as a function of the true strain during cold rolling.<sup>6</sup>

als<sup>15-19</sup> including polymers as will be discussed in the following sections.

In terms of the experiments this means that a wide angle X-ray diffractogram of the (semi) crystalline material has to be recorded with high angular and intensity resolution. Careful consideration and deconvolution of diffuse background and additional crystalline phases is crucial for the following evaluation. This can be followed by a correction of the instrumental broadening by a Stokes correction.<sup>20</sup> Only now the physical models described in this section can be fitted to the preprocessed data using an appropriate software (MWP-fit and CMWP-fit for the present work<sup>21</sup>).

## EXAMPLES OF APPLICATION

### Dislocation governed plasticity in $\alpha$ -iPP

The ability of MXPA to measure the dislocation density in arbitrary crystalline matter suggests to apply this method to semicrystalline polymers to gain insight into the role of dislocations in this class of materials. For a general applicability of the method, sufficient information on the anisotropic strain field of the expected causes for the broadening is mandatory, i.e., a sufficient number of linearly independent Bragg reflections in the diffractogram is required. This condition led to the choice of  $\alpha$ -crystallized polypropylene as a model material where a first investigation<sup>6,22</sup> combining modified Williamson-Hall analysis<sup>23</sup> with MXPA<sup>21</sup> could be achieved. Diffraction patterns were recorded on cold rolled samples revealing an increase of the dislocation density from initially  $3.8 \times 10^{16} \text{ m}^{-2}$  to  $7.3 \times 10^{17} \text{ m}^{-2}$  after deformation up to a true strain of  $\varepsilon_t = 0.5$  (Fig. 1).

Although these values might appear as rather high (coarse-grained metals show values of the order

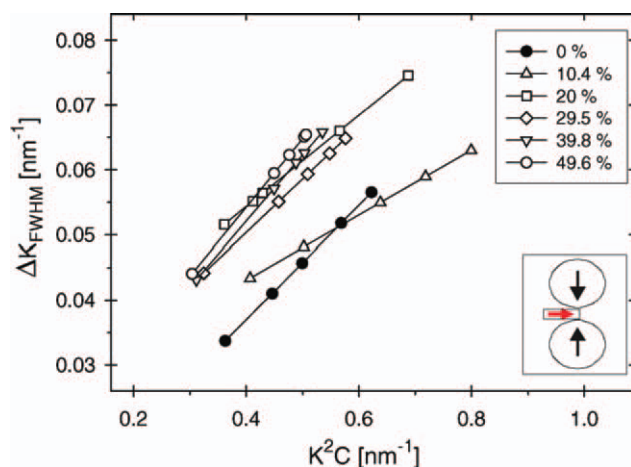


**Figure 2** Modified Williamson–Hall plot of  $\alpha$ -iPP deformed up to true strains of  $\varepsilon_t = 0.50$  achieved by cold rolling.<sup>6</sup> [Color figure can be viewed in the online issue, which is available at [wileyonlinelibrary.com](http://wileyonlinelibrary.com).]

of  $10^{13} - 10^{14} \text{ m}^{-2}$ ), the amount of dislocations necessary to provide a plastic deformation of  $\varepsilon_t = 0.5$  corresponds to a dislocation density in the order of  $10^{16} \text{ m}^{-2}$  when assuming a mean free path of dislocations in the order of the lamella thickness.<sup>6</sup> An upper limit for the possible dislocation density was given by Séguéla<sup>23</sup> with a value of  $10^{18} \text{ m}^{-2}$  based on thermal dislocation generation on lamella surfaces.<sup>25</sup> The experimental results of Wilhelm et al.<sup>6</sup> are within both of these estimations.

The dislocation mediated origin of the strain-broadening could be shown using the Williamson and Hall method and its modified version. Plotting the full width at half maximum of the peaks as a function of their diffraction vector  $k$  allows for a separation of the effects of size and strain broadening. Deviations from a monotonous behavior point at the presence of anisotropic strains. The modified Williamson–Hall plot accounts for the dislocation specific broadening through the average contrast factor for dislocations  $\bar{C}$ . Therefore a monotonous behavior of the FWHM as a function of  $k^2 \bar{C}$  in the modified Williamson-Hall plot (Fig. 2) is a very strong evidence for the presence of dislocations. These investigations were the first direct proof and quantification of dislocations in a melt crystallized polymer.

#### Lamella thickness in $\alpha$ -iPP

Also in  $\alpha$ -iPP the lamella thickness distribution was investigated by means of MXPA and compared to lamella thickness distributions with log-normal characteristics obtained by differential scanning calorimetry (DSC). The sizes of the coherently scattering domains (CSD, the smallest undistorted crystal areas which are determined by the diffraction experiment) are compared to the stem lengths (the distance of

two adjacent fold surfaces along the molecular chain provided by the DSC measurement). Under consideration of dislocations, both distributions coincide very well (Fig. 3) which is not the case if only little or no crystal defects, i.e., dislocations, are assumed for the MXPA. Therefore, crystalline defects have to be considered for a correct determination of the size distribution of semicrystalline polymers by MXPA. The good agreement between X-ray and DSC results suggests to use DSC to determine reasonable starting parameters for MXPA or even to calculate  $A^S(L)$  directly from the DSC size distribution.<sup>7</sup> The relatively low initial dislocation density of about  $10^{14} \text{ m}^{-2}$  seems to be a consequence of the annihilation of dislocations during the treatment preceding the experiment. The injection-molded samples used by Wilhelm et al.<sup>6</sup> contained a certain degree of internal stress presumably stabilizing dislocations, thus leading to higher dislocation densities.

#### Mechanism of plasticity in P3HB

The considerable deformation-induced increase of the dislocation density in polypropylene suggested to investigate the respective behavior of other semicrystalline polymers. The need for several strong Bragg reflections together with a high degree of crystallinity restricts the number of possible materials, but the biodegradable polymer poly(3-hydroxybutyrate) (P3HB) fulfills this condition.

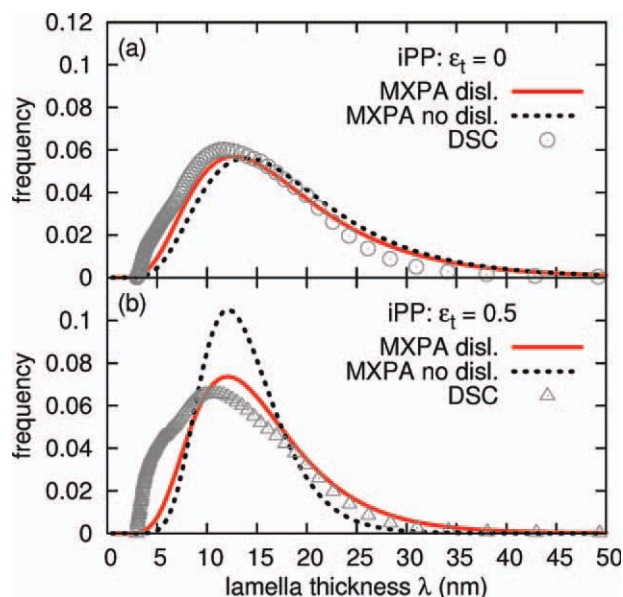


**Figure 3**  $\alpha$ -iPP undeformed and deformed to a true strain of  $\varepsilon_t = 0.50$  investigated by means of MXPA and DSC. (a) In the undeformed sample the results of MXPA coincide well with the DSC measurement. (b) Crystalline defects have to be taken into account for the MXPA evaluation to achieve a correct CSD-size distribution for the deformed material.<sup>7</sup> [Color figure can be viewed in the online issue, which is available at [wileyonlinelibrary.com](http://wileyonlinelibrary.com).]

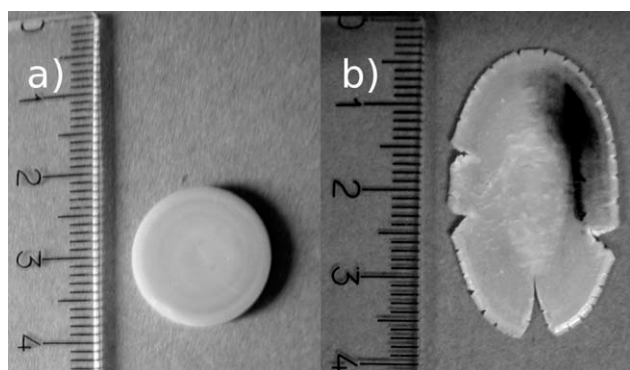


**Figure 4** P3HB cold rolling samples (a) undeformed and (b) deformed up to an engineering strain of  $\varepsilon = 0.62$  showing whitening and cracking at the edges.

*In situ* diffraction was carried out during uniaxial compression of P3HB at the SAXS Beamline of Synchrotrone Trieste in Italy.<sup>8</sup> Cold rolled samples were also studied *ex situ* (Figs. 4 and 5) to check for potential effects caused by the inhomogeneous deformation arising with the compression tests. The samples were deformed up to engineering strains of  $\varepsilon = 0.45$  in compression and up to  $\varepsilon = 0.75$  by rolling. The resulting relative dislocation densities for both experiments are shown in Figure 6 and compared with the characteristics of  $\alpha$ -iPP. Dislocation densities of the order of  $6.5 \times 10^{16} \text{ m}^{-2}$  were found in the as-extruded material.

It is quite remarkable that the dislocation density as determined by MXPA is not affected by plastic deformation. Within a certain scattering, also the CSD-size stays constant. Reasonable agreement of size distributions from DSC (bimodal) and from MXPA (assumed log-normal) shown in Figure 7 underline the reliability of these results. Hence in P3HB no deformation induced X-ray line broadening is observed. This is in accordance with the absence of changes in the crystallographic texture with plastic deformation (the relative peak intensities in Figure 5 stay constant), and a rather strong reduction of the crystallinity. This suggests a deformation

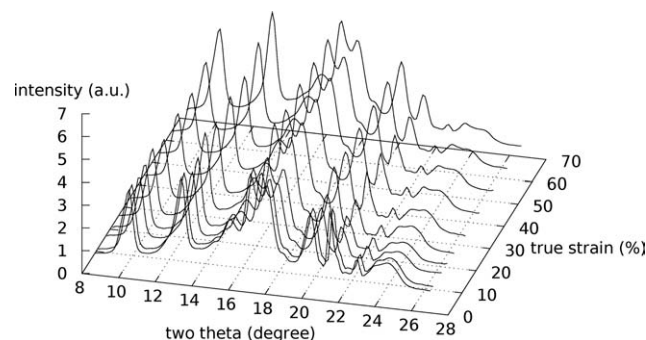


**Figure 5** Diffraction pattern of compressed P3HB deformed to true strains of  $\varepsilon_t = 0.75$ .

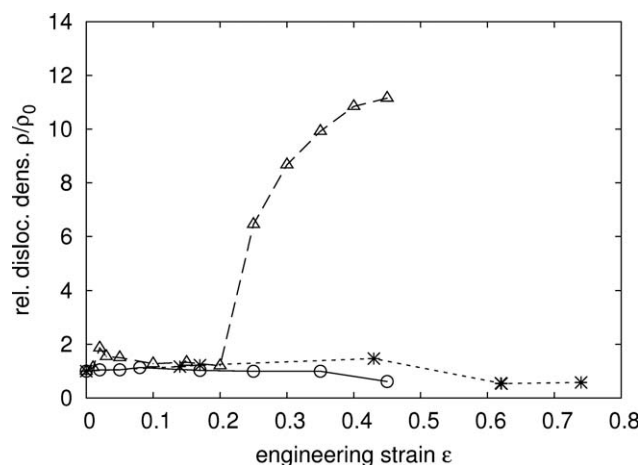


**Figure 6** Evolution of the relative dislocation densities of P3HB for uniaxial compression ( $\circ$ ,<sup>8</sup>) and cold rolling ( $*$ , this work) as a function of the engineering strain. In contrast to uniaxially compressed  $\alpha$ -iPP ( $\Delta$ ,<sup>8</sup>) no increase is induced by plastic deformation.

mechanism to be active different from dislocation-mediated crystallographic slip.

Possible alternative deformation mechanisms include (a) adiabatic melting and recrystallization of the lamellae<sup>3</sup> (b) concentration of the deformation in interlamellar areas, and subsequent fragmentation of the lamellae before crystallographic slip occurs. The marked brittleness of the bulk material shown in Figure 4, and the formation of microcracks at early stages of deformation (Fig. 8) also hint at the occurrence of such a process.

It should be noted that the behavior of P3HB has been—to some extent—also observed in the  $\gamma$ -phase of polypropylene where the arrangement of the molecular chains<sup>26</sup> considerably reduces the number of possible slip systems.<sup>27,28</sup> Recent investigations of the authors in  $\gamma$ -iPP indeed reveal an only small

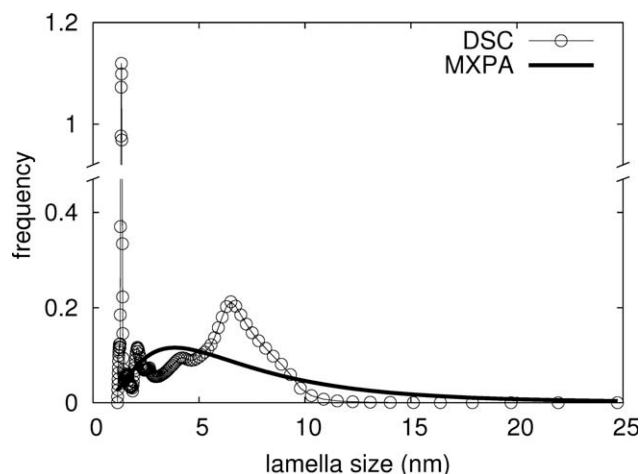


**Figure 7** Lamella size distribution of undeformed P3HB as determined by DSC and MXPA (using the lognormal model).

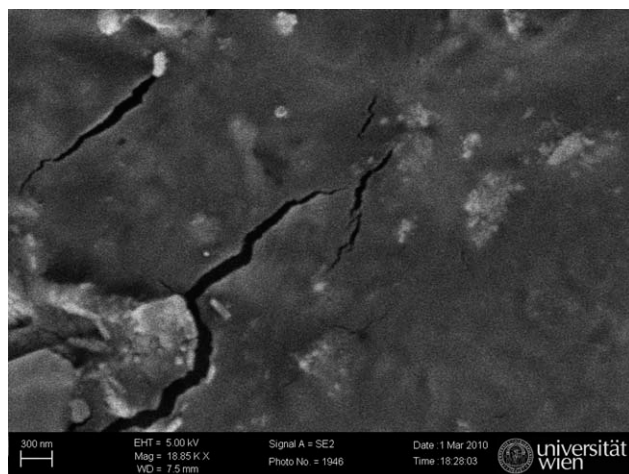


**Figure 8** Scanning electron micrograph showing already considerable crack formation at early stages of deformation ( $\epsilon = 0.17$ ).

increase in the dislocation density, corresponding to some need for geometrically necessary misfit dislocations which accommodate lamellar bending<sup>29</sup>

## SUMMARY AND CONCLUSIONS

While the microstructural changes during plastic deformation, i.e., the development of the crystalline texture, the fragmentation of crystals (=lamellae), and the formation of highly oriented structures were fairly clarified so far, the mechanical behavior of semicrystalline polymers is not understood yet. Reasons for this are the complex structure (amorphous and crystalline phases, spherulitic superstructures, tie molecules), and the interplay of strong bonding forces within the macromolecules and the much weaker Van der Waals bonds between the molecules.

If one compares the possible micromechanical processes as localized melting, shear of atomic crystal planes, and dislocation motion, the latter proves to be energetically the most favorable one. Dislocations have been shown to account very well for the experimental observations in a number of semicrystalline polymers. Making use of their characteristic strain field, the method of Multiple Whole Profile Analysis (MXPA) revealed to be capable of investigating the presence and density of dislocations. In general, the method has a high potential for analyzing semicrystalline polymers, although there may be some obstacles for the application in some materials as the restricted number and overlapping of X-ray reflections.

In this article MXPA was presented as an experimental technique to investigate important micromechanical parameters such as the lamella thickness and its distribution, as well as the dislocation density, in the semicrystalline polymers iPP and P3HB.

The experimental results reveal a considerable difference of P3HB and iPP with respect to the mechanism of plastic deformation; while dislocation generation can be observed in MXPA experiments of deformed iPP, this is not the case for P3HB. The high macroscopic and microscopic tendency of P3HB to form cracks together with the constant dislocation density evolution conform to a high strength of the crystalline phase, leading to destruction of the crystalline lamellae before dislocation mediated slip can occur.

In conclusion dislocation mediated plasticity can be considered as a process which might apply to some but not to all semicrystalline polymers.

## References

1. Young, R. J. *Philos Mag* 1974, 30, 85.
2. Shadrake, L. G.; Guiu, F. *Philos Mag* 1976, 34, 565.
3. Flory, P. J.; Yoon, D. Y. *Nature* 1978, 272, 226.
4. Seguela, R. *e-Polymers* 2007, 032.
5. Galeski, A.; Bartczak, Z.; Kazmierczak, T.; Slouf, M. *Polymer* 2010, 51, 5780.
6. Wilhelm, H.; Paris, A.; Schafler, E.; Bernstorff, S.; Bonarski, J.; Ungar, T.; Zehetbauer, M. *J Mater Sci Eng A* 2004, 387–389, 1018.
7. Spieckermann, F.; Wilhelm, H.; Schafler, E.; Kerber, M.; Bernstorff, S.; Zehetbauer, M. *J Phys Conf Ser* 2010, 240, 012146.
8. Spieckermann, F.; Wilhelm, H.; Kerber, M.; Schafler, E.; Polt, G.; Bernstorff, S.; Addiego, F.; Zehetbauer, M. *J Polymer* 2010, 51, 4195.
9. Kerber, M. B.; Zehetbauer, M. J.; Schafler, E.; Spieckermann, F. C.; Bernstorff, S.; Ungar, T. *JOM* 2011, 63, 61.
10. Warren, B. E.; Averbach, B. L. *J Appl Phys* 1950, 21, 595.
11. Warren, B. E.; Averbach, B. L. *J Appl Phys* 1952, 23, 497.
12. Krivoglaz, M. A. *Theory of X-Ray and Thermal Neutron Scattering by Real Crystal*; Plenum: New York, 1969.
13. Wilkens, M. *Phys Stat Sol* 1987, 104, K1.
14. Klimanek, P.; Kuzel, R. *J Appl Crystallogr* 1988, 21, 59.
15. Ungar, T.; Schafler, E.; Gubicza, J. In *Bulk Nanostructured Materials*; Zehetbauer, M. J., Zhu, Y. T., Ed.; Wiley-VCH: Weinheim, 2009; Chapter 17, pp 361–386.
16. Ungar, T. In *Defect and Microstructure Analysis by Diffraction*; Snyder, R., Fiala, J., Bunge, H. Ed.; Oxford University Press: Oxford, 1999; Chapter 10, pp 165–199.
17. Ungar, T. *Adv Eng Mater* 2003, 5, 323.
18. Leoni, M.; Scardi, P. *J Appl Crystallogr* 2004, 37, 629.
19. Scardi, P.; Leoni, M. *Acta Crystallogr A* 2002, 58, 190.
20. Kerber, M.; Schafler, E.; Zehetbauer, M. *Rev Adv Mater Sci* 2005, 10, 427.
21. Ribarik, G.; Ungar, T.; Gubicza, J. *J Appl Crystallogr* 2001, 34, 669.
22. Paris, A. *Anwendung der Bragg-Profilanalyse zur Bestimmung von verformungsinduzierten Versetzungen in Polypropylen*. Diploma Thesis, University of Vienna, 2003.
23. Ungar, T.; Borbely, A. *Appl Phys Lett* 1996, 69, 3173.
24. Seguela, R. *J Polym Sci B* 2002, 40, 593.
25. Peterson, J. M. *J Appl Phys* 1968, 39, 4920.
26. Meille, S. V.; Bruckner, S.; Porzio, W. *Macromolecules* 1990, 23, 4114.
27. Lezak, E.; Bartczak, Z.; Galeski, A. *Macromolecules* 2006, 39, 4811.
28. Lezak, E.; Bartczak, Z. *Macromolecules* 2007, 40, 4933.
29. Polt, G. *Mechanisms of Plastic Deformation in  $\gamma$ -Isotactic Polypropylene*. Diploma Thesis, University of Vienna, 2011.